SUPPLEMENTARY MATERIAL

Title: Neurodegenerative disease-associated mutants of a human mitochondrial aminoacyl-tRNA synthetase present individual molecular signatures

Author list: Claude SAUTER[1†]*, Bernard LORBER[1†], Agnès GAUDRY[1], Loukmane KARIM[1], Hagen SCHWENZER[1#], Frank WIEN[2], Pierre ROBLIN[2,3], Catherine FLORENTZ[1] and Marie SISSLER[1]*

[1] Architecture et Réactivité de l'ARN, CNRS, Université de Strasbourg, IBMC, 15 rue René Descartes, 67084 STRASBOURG Cedex, France

[2] Synchrotron SOLEIL, L'Orme des Merisiers Saint Aubin, 91410 Gif-sur-Yvette, France;

[3] URBIA-Nantes, INRA Centre de Nantes, 60 rue de la Géraudière, 44316 Nantes, France.

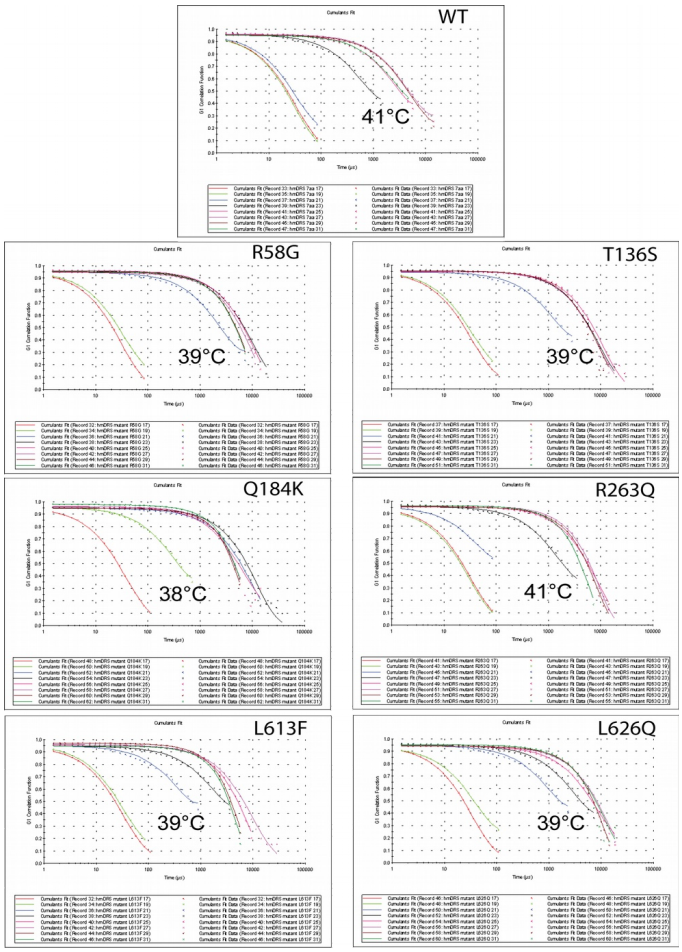

Supplementary Figure 1: DLS analysis of WT mt-AspRS and mutants as a function of temperature. A shift in the auto-correlation function indicates a drop in diffusion coefficient (i.e. increase in size). The temperature at which the shift starts is highlighted.

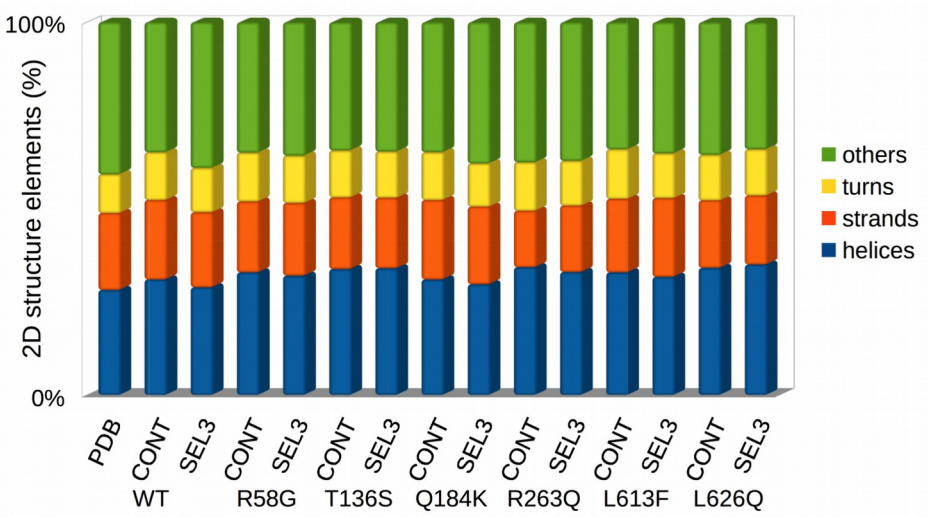

Supplementary Figure 2: Secondary structure contents of WT mt-AspRS and mutants. The percentage of helices, beta strands and turns was determined from SRCD spectra collected at 24°C (as displayed in Figure 2) using CONTINLL and SELCON3 (see methods). The distribution of 2D elements in the X-ray structure of mt-AspRS (PDBid: 4AH6) was determined using DSSP[49]. Numerical data are listed in **Supplementary Table 2**.

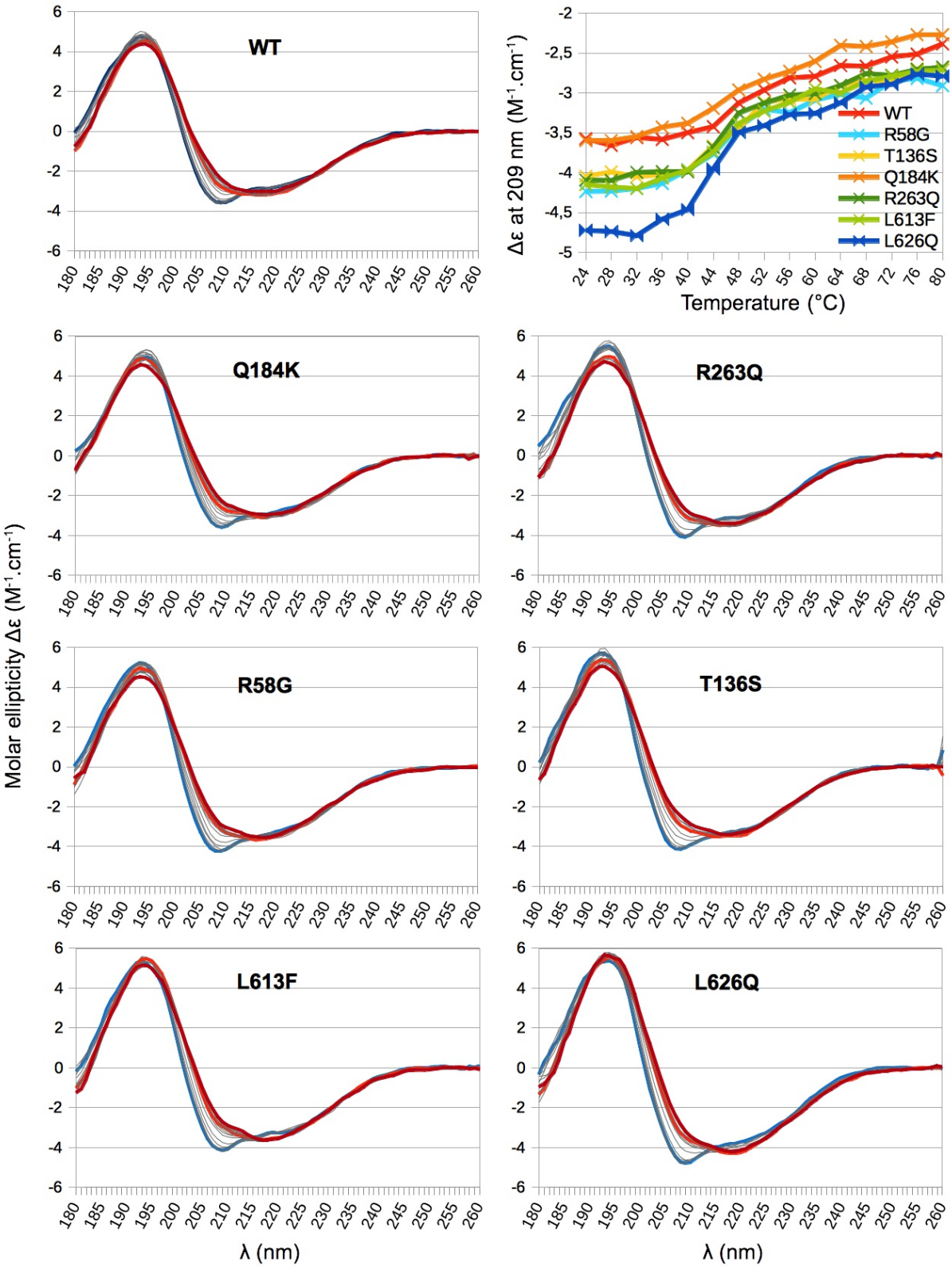

Supplementary Figure 3: SRCD spectra of WT mt-AspRS and mutants as a function of temperature. The temperature was stepwise increased from 24°C (blue curve) to 80°C (red curve). (Top right panel) Variation of ellipticity at 209 nm is plotted for each variant as a function of temperature.

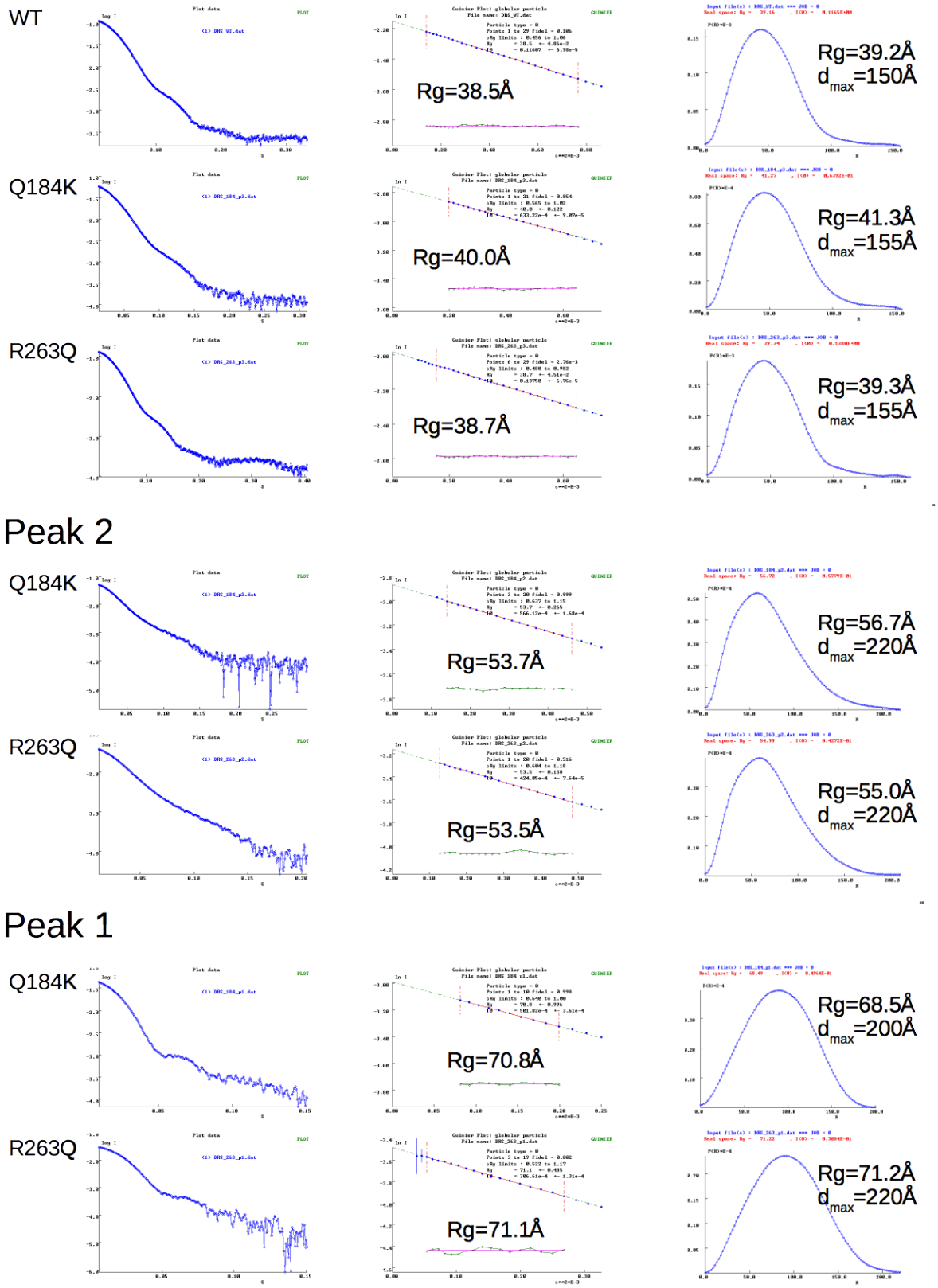

Supplementary Figure 4: SAXS analysis of WT mt-AspRS and Q184K and R263Q mutants. (Left, center, right) Experimental SAXS profiles, Guinier plots and P(r) distance distribution functions for each protein population isolated by SEC in peaks 1-3.

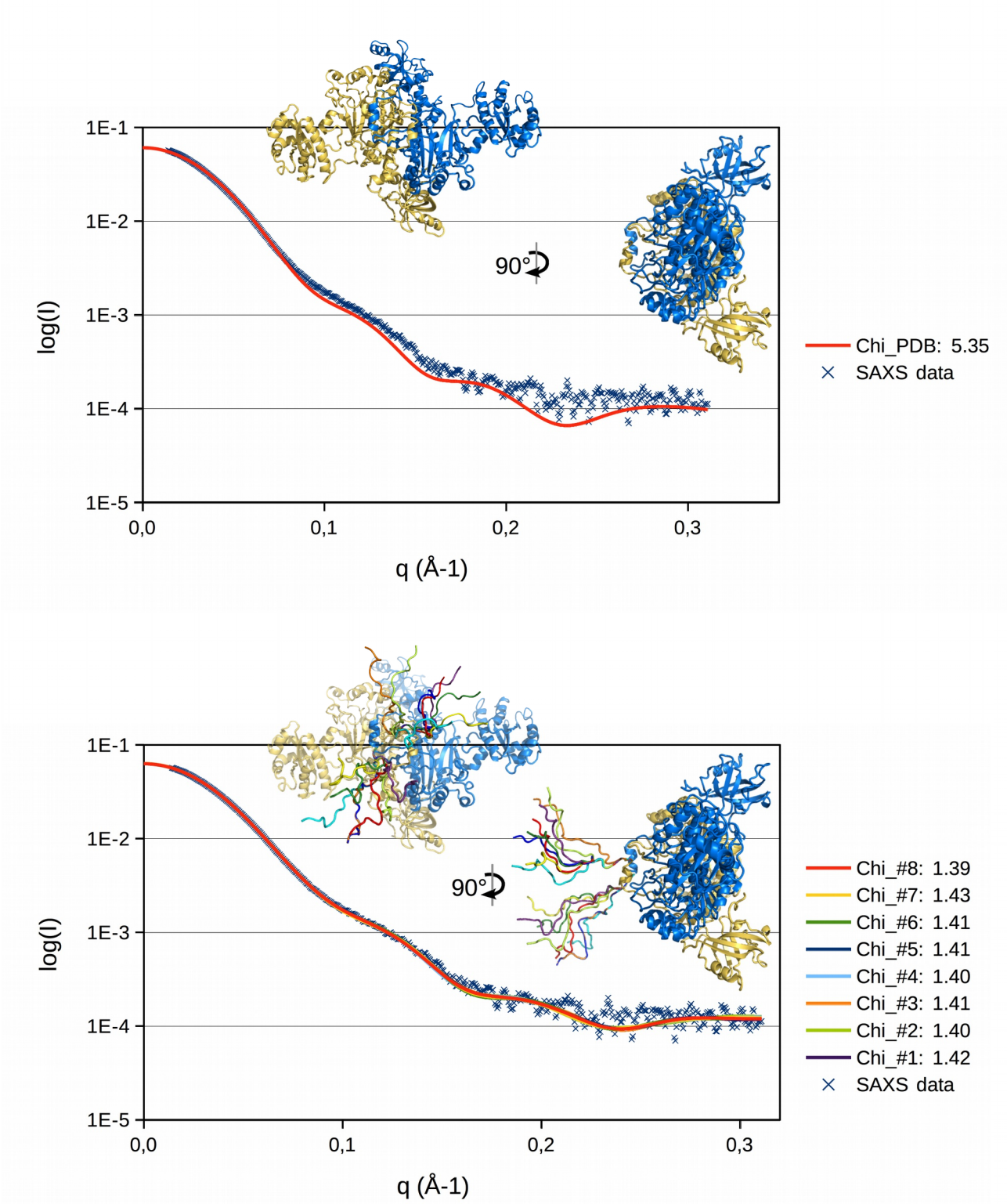

Supplementary Figure 5: Structure of mt-AspRS dimers in solution. Experimental SAXS profile of mtAspRS (Q184K mutant - blue dots) was compared to theoretical curves computed for atomic models corresponding to the crystal structure (PDBid: 4AH6) lacking the C-terminal extensions (Top) and to a series of complete models generated by DADIMODO (Bottom). C-terminal extension models and corresponding curves are depicted with the same color. The goodness-of-fit (Chi) was determined using CRYSOL. Models including the C-terminal extensions display a better fit with the data as indicated by lower Chi values.

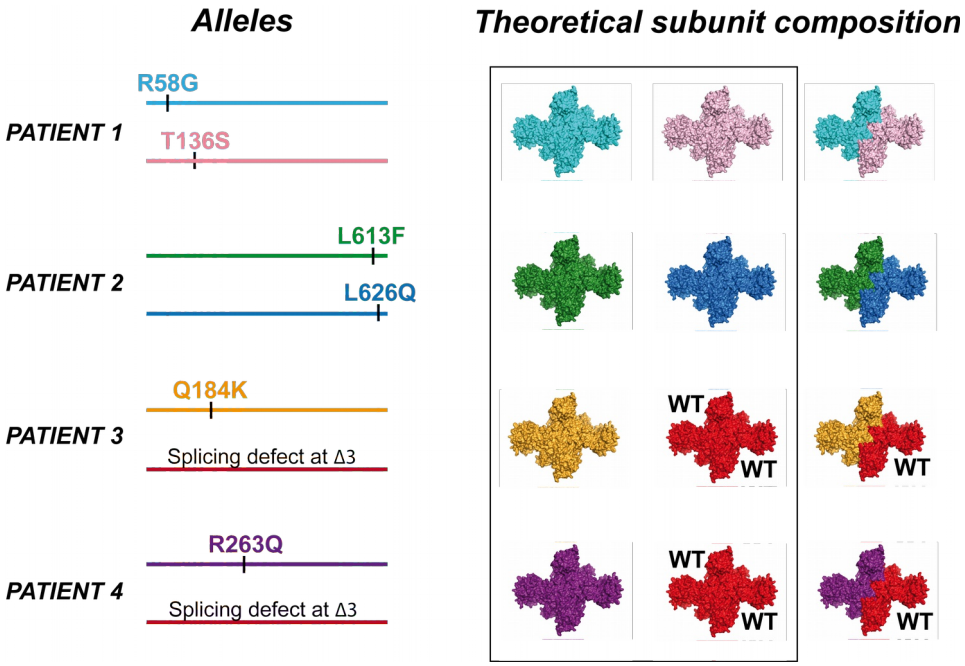

Supplementary Figure 6: Theoretical subunit composition of mt-AspRS dimers resulting from LBSL associated mutations in alleles of heterozygote patients. Situations explored in this study are boxed.

Supplementary Table 1: Phenotypes of LBSL patients with selected mutations

Allelic composition		First neurological Signs at years	Loss of unsupported walking at years	Full wheelchair dependency at years	Age in 2013 in years
Mutation 1	Mutation 2				
R58G	T136S	3	-	-	23
R58G	T136S	2	-	-	15
L613F	L626Q	12	28	-	36
Q184K	R76Serfs*5	6	-	-	22
Q184K	R76Serfs*5	7	18	-	20
R263Q	R76Serfs*5	3	8	20	33
R263Q	R76Serfs*5	5	28	-	29
R263X [a)]	R76Serfs*5	2	6	-	20
R263X [a)]	R76Serfs*5	1	14	22	24

Adapted from [50]. [a)] not analyzed in the present study but added for comparison.

Supplementary Table 2: Secondary structure contents derived from SRCD spectra

Sample		**WT-mt-AspRS**	**R58G**	**T136S**	**Q184K**	**R263Q**	**L613F**	**L626Q**
Method	PDB	CONT / SEL3	CONT / SEL3	CONT / SEL3	CONT / SEL3	CONT / SEL3	CONT / SEL3	CONT / SEL3
Helices	28,2	31,0 / 28,9	32,9 / 32,0	33,8 / 34,0	31,0 / 29,7	34,3 / 33,0	32,9 / 31,7	34,1 / 35,0
Strands	20,6	21,3 / 20,1	19,0 / 19,5	19,2 / 18,9	21,3 / 20,8	15,1 / 17,8	19,7 / 21,1	18,1 / 18,5
Turns	10,4	12,8 / 11,9	13,1 / 12,7	12,6 / 12,4	12,8 / 11,6	13,0 / 12,0	13,3 / 12,0	12,2 / 12,4
Others	40,8	34,9 / 39,1	35,0 / 35,8	34,4 / 34,7	34,9 / 37,9	37,6 / 37,2	34,1 / 35,2	35,6 / 34,1
RMSD		9,8 / 14,6	0,1 / 12,2	13,1 / 12,8	9,8 / 14,6	13,0 / 19,0	12,2 / 13,5	13,9 / 13,4

The percentage of 2D elements was assessed from the PDB entry of WT mt-AspRS using DSSP [49] and determined from SRCD spectra collected at 24°C using CONTINLL (CONT) and SELCON3 (SEL3). The RMSD of the 2D element estimation is indicated for each method.

Supplementary Table 3: Analysis of amino acid conservation and changes in mt-AspRS sequences

Mutations		**R58G**	**T136S**	**Q184K**	**R263Q**	**L613F**	**L626Q**
Location		Anticodon-binding domain	Anticodon-binding domain	Catalytic domain	Catalytic domain	C-terminal extension	C-terminal extension
conservationWT residue	**all seq.** (180)	no	no	no	**R/K** (~97%)	no	no
	mt mammals (11)	mainly **R**	yes	yes	yes	only **L/V**	yes
	mt others (49)	no	no	no	mainly **R**	**L** (~60%), **P** (~40%)	**L** (~80%), **R** (~20%)
	bacteria (120)	no	mainly **T** – a few **S**	no	mainly **R**	**L** (~60%), **P** (~40%)	**L** (~80%), **R** (~20%)
Natural occurrence of substituting residue		**G** in some bacteria	**S** in some bacteria	**R/K** in some bacteria; **R** in mt of fungi	**Q** in one bacterium and one mt arthropod	no	no
Structural environment of WT residue		Exposed to solvent. No visible interaction with neighbor residues	Hydrophobic environment. Near **L**, **V** and **M** residues	At the beginning of dimerization helix. Involved in a network of hydrogen bonds (G253 from other chain; L178 and R188 of the same chain)	Close to the enzyme 2-fold axis. Interacts with E277 (from same monomer) and T212 (from opposite monomer)	In the vicinity of tRNA binding site	Close to the enzyme 2-fold axis. In the dimerization mini-helix
Theoretical structural impact of the mutation		Loss of one positive charge. No local rearrangement	Loss of a methyl group and of van der Waals interactions, but compatible with hydrophobic environment.	15 out of 18 theoretical conformers lead to steric hindrances.	Loss of a positive charge. Leaves a negative charge with no interactant	2 out of 4 theoretical conformers lead to steric hindrances.	4 out of 16 theoretical conformers lead to steric hindrances.

–Conservation of WT residue– and –Natural occurrence of substitution– were analyzed in a multiple sequence alignment composed of 180 bacterial–type AspRSs, as generated in[51]. This alignment is made of 120 sequences of AspRS proteins from bacteria (encompassing all bacterial subgroups) and 60 sequences of mt-AspRS proteins from eukaryotes (with representatives of mammals, arthropods, fungi and protists). For an objective evaluation of the sequence conservation or divergence, redundancy was avoided by considering only non-identical sequences.

Supplementary Table 4: Analysis of amino acid conservation of mt-AspRS positions impacted by disease-associated missense mutations

	Mutations	**N52S** (ref.[50])	**R125H** (ref.[50])	**I139T** (ref.[50])	**C152F** (ref.[52])	**R179H** (ref.[52])	**G206E** (ref.[50])	**L239P** (ref.[53])	**Q248K** (ref.[52])	**L249I** (ref.[54])
	Location	anticodon-binding domain	anticodon-binding domain	anticodon-binding domain	anticodon-binding domain	helix of dimerization	catalytic domain (motif 1)	catalytic domain	catalytic domain	catalytic domain
conservationWT residue	**all seq. (180)**	no	**R/K** (~97%)	no	no	yes (100%)	no	yes (100%)	yes (100%)	no
	mt mammals (11)	**yes (100%)**	**yes (100%)**	**yes (100%)**	**yes (100%)**	**yes (100%)**	**yes (100%)**	**yes (100%)**	**yes (100%)**	**yes (100%)**
	mt others (49)	no	no (mainly **K**)	no	no	yes (100%)	no	yes (100%)	yes (100%)	no (**L/I/M/T**)
	bacteria (120)	no (never a **N**)	yes (100% **R**)	mainly **I/V**	no	yes (100%)	no	yes (100%)	yes (100%)	no (**L/I/M/V**)
	natural occurrence of substituting res.	no	no	no	no	no	**E** in some mt others, and in some bacteria	no	no	**I** in some mt others, and in some bacteria
	allelic composition	**C152F**	Exon 3 splicing defect	Exon 3 splicing defect	**N52S**	Exon 3 splicing defect	Exon 3 splicing defect	Exon 3 splicing defect	Exon 3 splicing defect	Exon 3 splicing defect

	Mutations	**L250P** (ref.[50])	**G254S** (ref.[50])	**E284K** (ref.[55])	**R336H** (ref.[50])	**P576S** (ref.[50])	**D560V** (ref.[52])	**R609W** (ref.[56])	**L626V** (ref.[52])	**Y629C** (ref.[52])
	Location	catalytic domain	catalytic domain	catalytic domain (motif 2)	catalytic domain	catalytic domain	catalytic domain	bacterial-type C-terminal extension	bacterial-type C-terminal extension	bacterial-type C-terminal extension
conservationWT residue	**all seq. (180)**	**L** (~97%)	**G** (~97%)	yes (100%)	**R** (~97%)	yes (100%)	no	no	no	no
	mt mammals (11)	**yes (100%)**	**yes (100%)**	**yes (100%)**	**yes (100%)**	**yes (100%)**	**yes (100%)**	**yes (100%)**	**yes (100%)**	**yes (100%)**
	mt others (49)	yes (100%)	mainly **G** (some **S/A**)	yes (100%)	mainly **R** (some **C/G**)	yes (100%)	no	no	no	yes (100%)
	bacteria (120)	mainly **L** (some **M/C**)	yes (100%)	yes (100%)	yes (100%)	yes (100%)	no	no	no	no
	natural occurrence of substituting res.	no	no	no	no	no	no	no	no	no

allelic composition	Exon 3 splicing defect	Exon 3 splicing defect	Exon 3 splicing defect	Exon 3 splicing defect	Exon 3 splicing defect	Exon 3 splicing defect	**R609W**	**L613F**	Exon 3 splicing defect

Mutations were taken from references [50, 52-56] as indicated. They were reported after the beginning of the present work (except for those from ref. [52]). –Conservation of WT residue– and –Natural occurrence of substitution– were analyzed in a multiple sequence alignment composed of 180 bacterial–type AspRSs, as generated in [51]. This alignment is made of 120 sequences of AspRS proteins from bacteria (encompassing all bacterial subgroups) and 60 sequences of mt-AspRS proteins from eukaryotes (with representatives of mammals, arthropods, fungi and protists). For an objective evaluation of the sequence conservation or divergence, redundancy was avoided by considering only non-identical sequences. Allelic composition recalls the situation found in patients.

References

49. Joosten, R.P. et al. A series of PDB related databases for everyday needs. *Nucleic Acids Research* **3**, D411-D419 (2011).
50. van Berge, L. et al. Leukoencephalopathy with brainstem and spinal cord involvement and lactate elevation: clinical and genetic characterization and target for therapy. *Brain* **137**, 1019-1029 (2014).
51. Schwenzer, H. et al. Released selective pressure on a structural domain gives new insights on the functional relaxation of mitochondrial aspartyl-tRNA synthetase. *Biochimie (Special Issue "Mitochondria: an organelle for life")* **100**, 18-26 (2014).
52. Scheper, G.C. et al. Mitochondrial aspartyl-tRNA synthetase deficiency causes leukoencephalopathy with brain stem and spinal cord involvement and lactate elevation. *Nat Genet* **39**, 534-539 (2007).
53. Lin, J. et al. Leukoencephalopathy with brainstem and spinal cord involvement and normal lactate: a new mutation in the DARS2 gene. *J. Child. Neurol.* **25**, 1425-1428 (2010).
54. Labauge, P., Dorboz, I., Eymard-Pierre, E., Dereeper, O. & Boespflug-Tanguy, O. Clinically asymptomatic adult patient with extensive LBSL MRI pattern and DARS2 mutations. *J. Neurol.* **258**, 335-337 (2011).
55. Cheng, F.B. et al. Adult-onset leukoencephalopathy with brain stem and spinal cord involvement in Chinese Han population: a case report and literature review. *Neurol India.* **61**, 161-163 (2013).
56. Synofzik, M. et al. Acetazolamide-responsive exercise-induced episodic ataxia associated with a novel homozygous DARS2 mutation. *J. Med. Genet.* **48**, 713-715 (2011).